Dynamic Patches of Membrane Proteins

Yael Lavi,* Michael A. Edidin,† and Levi A. Gheber*
*Department of Biotechnology Engineering, Ben-Gurion University of the Negev, Beer-Sheva, Israel; and †Department of Biology, Johns Hopkins University, Baltimore, Maryland USA

ABSTRACT We test here a previously proposed hypothesis about lateral heterogeneity of cell membranes, a model predicting that heterogenity is maintained by a combination of delivery and intake of molecules with barriers to lateral free diffusion. To test the validity of the model, we observed green florescent protein tagged major histocompatibility complex class I patches on the plasma membrane of mouse fibroblasts, using total internal reflection fluorescence microscopy in real time. The dynamic characterization revealed the life course of these patches comprises delivery of molecules at a short instant, followed by a slow, exponential decay, corresponding to diffusion of the molecules over dynamic barriers to free lateral diffusion. The characteristic lifetime of the patches, extracted from the measurements, is ~30 s, in excellent agreement with the predictions of the model.

Received for publication 26 April 2007 and in final form 28 June 2007.

Address reprint requests and inquiries to Levi A. Gheber, E-mail: glevi@bgu.ac.il.

Cell surface membranes of many cell types are typically patchy, strewn with heterogeneities whose composition and function differ from the average for an entire membrane. One type of microdomain present is a cluster of like membrane proteins. For example, the type I membrane proteins MHC-I molecules and erbB2 are in microdomains hundreds of nanometers in diameter (1–2). This size scale is commensurate with the spacing of the barriers to lateral mobility detected by lateral diffusion, single particle tracking, and laser trap experiments (3–6).

Although clustering of membrane proteins is likely to be energetically favored (7), it is not clear how protein-rich microdomains are maintained in the face of lateral diffusion and the transient opening of the barriers to lateral diffusion (4,8–9). We have proposed a quantitative model for patchy membranes (10) that suggests that these microdomains are maintained by a combination of vesicle trafficking to and from the cell surface, which leads to local concentrations of newly delivered membrane proteins, confinement of membrane proteins by dynamic barriers, and the dispersion of individual patches by lateral diffusion. The model of dynamic microdomains predicts a characteristic lifetime ~20 s for a given microdomain. The model also predicts that blocking vesicle traffic, will result in larger but dimmer patches of proteins, and this was observed for MHC-I patches after blocking clathrin-mediated endocytosis (11). However, although these studies characterized patch sizes, they did not capture the dynamics of patch dispersion.

Here we test the prediction of patch lifetime made by our model. We describe the dynamics of green florescent protein (GFP)-tagged major histocompatibility complex (MHC)-I molecules (12) in living cells using total internal reflection fluorescence microscopy (TIRFM) (13) to exclude fluorescence from the cell volume. Measurements of over 800 individual MHC-I patches gave a median lifetime of ~30 s, in good agreement with the predictions of the model. These results point to one mechanism by which microdomains are maintained on the cell surface and suggest a useful timescale for considering the interactions of ligands and cell receptors with clusters of membrane proteins. For example, the patch lifetimes that we measured are of the same order of magnitude as the time required for T-cell receptors to clusters in responses to antigen presented by MHC molecules (14).

All reagents were purchased from Biological Industries (Kibbutz Beit Haemek, Israel) unless otherwise noted. Normal mouse fibroblasts (L-M(tk^-)) expressing MHC-I, H2-Kb with their intracellular region tagged with GFP (GFP-in) (12). were cultured in 250 ml TC flasks (Cellstar, Grenier Bio-One, Frickenhausen, Germany) at 37°C and 5% CO_2 in Roswell Park Memorial Institute medium (RPMI-1640) without L-glutamine, with 10% fetal bovine serum, 0.22 mg/ml G418 (geniticin; Sigma, St. Louis, MO). For mounting, cells were detached from flasks by incubating in 2 ml trypsin EDTA 0.25% for 10 min at 37°C, and transferred to homemade glass bottom petri dishes, in 2 ml medium. After overnight incubation, medium was removed and dishes were gently rinsed 3 times and imaged in 2.5 ml warmed (37°C) Hepes Hanks' balanced salt solution. Imaging was carried out on a homemade prism-based TIRFM system, using an Argon-ion laser (35 MAP 321 from Melles Griot laser group, Carlsbad, CA) at 488 nm as the excitation light source. Cells were imaged with a SPOT charge-coupled device camera (Diagnostic Instruments, Sterling Heights, MI), mounted on a Zeiss (Jena, Germany) Axioplan2 upright light microscope with a 40×, 1.3 N.A. objective.

Total internal reflection illumination creates an evanescent field at the interface between glass and cell membrane that decays exponentially into the cell with a penetration depth of ~100 nm, thus exciting fluorescence primarily in the cell

Editor: Barry R. Lentz.

doi: 10.1529/biophysj.107.111567

membrane. In our setup fluorescence is excited in the lower membrane, which is adhered to the glass, and the emitted light is collected by an upright microscope. Fig. 1 compares the images obtained on the same cell in epi-fluorescence (Fig. 1 *A*) and TIRFM (Fig. 1 *B*). The microdomains are clearly visible in Fig. 1 *B*, owing to the exclusion of fluorescence from within the cell volume. Both images are taken in the same focal plane, however, the exposure in Fig. 1 *A* is much shorter, due to the bright fluorescence from the whole cell volume, which causes the cell edges to appear fuzzier.

Because the model predicts characteristic life times of ~20 s we imaged series of frames as in Fig. 1 *B* with equal exposure time per frame, for a total time of 2–5 min. Exposure times ranged between 1 and 5 s, depending on the brightness of the cell under investigation. Recording of frames was stopped when photobleaching caused the signal to decay below the noise level of the camera. These sampling frequencies should be appropriate to capture faithfully dynamics with this characteristic time. The intensity faithfully reports the relative number of molecules in a patch, however, the apparent size is diffraction limited. The size of such patches has been previously characterized using near-field scanning optical microscopy, to overcome the diffraction limit in far field, and was shown to be 300–700 nm in diameter (1).

Eight-hundred and eighty-two patches from 25 different cells, cultured in three different dishes, were individually analyzed, plotting their intensity as a function of time. The analysis on individual patches was performed following correction for photobleaching over the time course of sampling. Two representative examples of fluorescence intensity as a function of time are shown in Fig. 2. In some cases a continuous decay of the intensity was observed during the time course of the experiment (Fig. 2 *A*), whereas in other cases

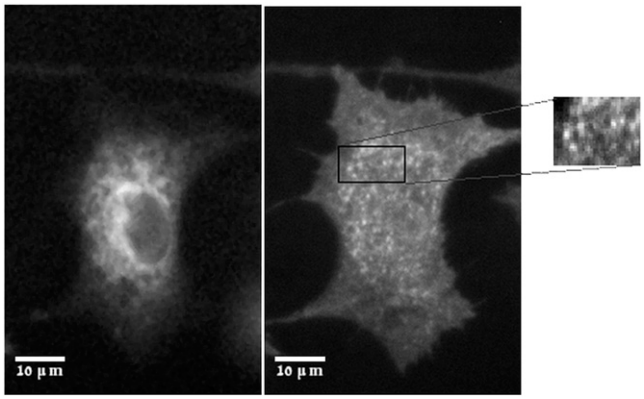

FIGURE 1 A cell expressing GFP-tagged MHC-I, imaged in two modes. (*A*) Conventional epi-fluorescence. (*B*) TIRFM. The dark nucleus is visible in panel *A*, surrounded by a bright region corresponding to the ER (*white arrow*). The MHC-I patches on the plasma membrane are clearly observed in panel *B*, as bright dots, and no fluorescence from the cell volume is excited: the ER is absent, the nucleus is not visible. (*C*) Zoom-in of the field indicated in panel *B*, showing some (diffraction limited) fluorescent patches.

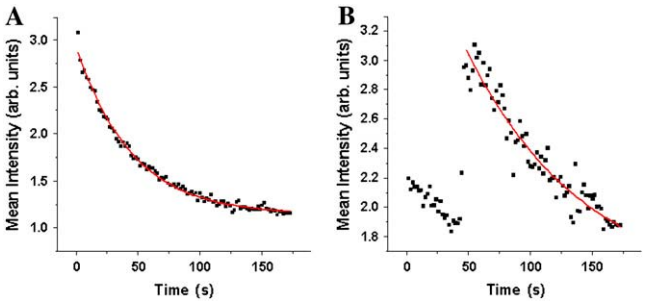

FIGURE 2 Fluorescence intensity of single patches, as a function of time, for two representative cases. (*A*) Continuously decaying intensity over the experiment duration. (*B*) A single sharp increase in fluorescence intensity preceded and followed by exponential decay. Solid lines represent best fit with a function of the form $I(t) = I_0 + A\ exp\ (-t/\tau)$.

one or two delivery events were captured during the sampling time (Fig. 2 *B*).

The solid lines represent best fits to a single exponential decay of the form $I(t) = I_0 + A\ exp\ (-t/\tau)$ where I_0 is the intensity at $t = \infty$ and τ is the characteristic lifetime of the patch. A movie is available as Supplementary Material.

All events as described in Fig. 1 *B* showed a similar behavior, consisting of a slowly decaying exponential and a much faster rise followed by a slowly decaying exponential (in a few cases two such consecutive rises were observed within the time course of the experiment). These events are interpreted as deliveries of MHC-I by vesicles fusing with the membrane, followed by an exponential decay due to diffusion of these restrained molecules over the dynamic barriers. In TIRFM, a vesicle approaching the membrane and departing from it would show an exponential dependence of its intensity over time (rising intensity while approaching the membrane, decreasing intensity while departing from it), due to the exponential variation of the excitation field in the *z*-direction, therefore it is important to rule out this possibility as a reason for our observations. A freely diffusing vesicle would show random intensity changes, both increasing and decreasing, with different time constants (no reason why vesicles would always approach fast and depart slowly), contrary to our measurements. In addition, free diffusion would have occurred in the *x*,*y* plane, as well as in the *z*-direction, however, the position of the fluorescent clusters was never observed to change over the time course of the experiment. If directed approach of vesicles is considered, by (unidirectional) molecular motors onto microtubules, this mechanism could be responsible for the fast intensity increase, whereas slow decay could be a result of the vesicle detaching from the microtubule shortly before fusion and diffusing freely away from the membrane. However, in this case, too, during the free diffusion phase, one should observe random time constants and alternative increase/decrease of intensity, accompanied by free diffusion in the *x*,*y* plane. This was never observed. Active transport toward the cell

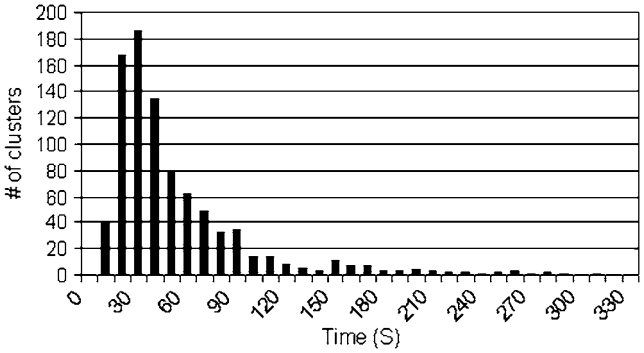

FIGURE 3 Distribution of characteristic lifetime of patches. The distribution is characterized by mean of 48 s and a median value of 32.7 s.

interior should occur with comparable velocities to transport toward the membrane, thus should appear as a fast decay, therefore it cannot explain the slow decay we are observing.

The reason we do not observe vesicles approaching and departing is due to the small penetration depth of our evanescent field. The shallow field penetration is further supported by images such as Fig. 1 *B*, where it is clear that even the endoplasmic reticulum (ER), which may be very close to the lower plasma membrane and is characterized by a very high fluorescence intensity (Fig. 1 *A*) due to high concentration of GFP-MHC-I, is not excited in the TIRFM images (Fig. 1 *B*). We thus conclude that we are observing new cargos of GFP-tagged MHC-I molecules being delivered to the plasma membrane; the molecules' fast diffusion is obstructed by the barriers to free lateral diffusion, therefore imposing a relative long lifetime of the elevated concentration patch.

The distribution of the characteristic lifetimes, extracted from fits as shown in Fig. 2 is plotted in Fig. 3. It has a mean of 48 s and a median value of 32.7 s, which is much more representative of the most probable value. This value is in excellent agreement with the aforementioned model, predicting ~20 s (10).

We observed dynamic behavior of MHC-I patches on the plasma membrane of cells, previously imaged directly using NSOM (1). The dynamics of these patches is characterized by a sharp increase in intensity, corresponding to a delivery—probably by an exocytic vesicle—followed by an exponential decrease in intensity due to diffusion of the molecules over dynamic barriers.

The characteristic lifetime of the patches is ~30 s, in very good agreement with the model predicting this behavior (10).

The observation of consecutive events as in Fig. 2 *B* in the same position indicates that delivery occurs at specific, nonrandom points on the membrane, a scenario that favors patchiness, when compared with random distribution of the delivery locations. Destabilizing the barriers is expected to result in reduction of the characteristic lifetime of the patches, while blocking vesicle traffic should result in larger and dimmer patches and lower frequency of delivery events, as described in Fig. 2 *B*. Modulating the size and nature of the patches may, in turn, modulate the response of T cells.

SUPPLEMENTARY MATERIAL

To view all of the supplemental files associated with this article, visit www.biophysj.org.

ACKNOWLEDGMENTS

The authors acknowledge Rudi Sokuler and Ram Gal for their support.

This work was supported in part by grant No. 1999257 from the U.S.-Israel Binational Science Foundation and grant No. AI14584 from the National Institutes of Health.

REFERENCES and FOOTNOTES

1. Hwang, J., L. A. Gheber, L. Margolis, and M. Edidin. 1998. Domains in cell plasma membranes investigated by near-field scanning optical microscopy. *Biophys. J.* 74:2184–2190.
2. Nagy, P., A. Jenei, A. K. Kirsch, J. Szollosi, S. Damjanovich, and T. M. Jovin. 1999. Activation-dependent clustering of the erbB2 receptor tyrosine kinase detected by scanning near-field optical microscopy. *J. Cell Sci.* 112:1733–1741.
3. Yechiel, E., and M. Edidin. 1987. Micrometer-scale domains in fibroblast plasma-membranes. *J. Cell Biol.* 105:755–760.
4. Edidin, M., S. C. Kuo, and M. P. Sheetz. 1991. Lateral movements of membrane-glycoproteins restricted by dynamic cytoplasmic barriers. *Science.* 254:1379–1382.
5. Sako, Y., and A. Kusumi. 1995. Barriers for lateral diffusion of transferrin receptor in the plasma-membrane as characterized by receptor dragging by laser tweezers—fence versus tether. *J. Cell Biol.* 129:1559–1574.
6. Saxton, M. J., and K. Jacobson. 1997. Single-particle tracking: applications to membrane dynamics. *Annu. Rev. Biophys. Biomol. Struct.* 26:373–399.
7. Matthews, E. E., M. Zoonens, and D. M. Engelman. 2006. Dynamic helix interactions in transmembrane signaling. *Cell.* 127:447–450.
8. Edidin, M., and I. Stroynowski. 1991. Differences between the lateral organization of conventional and inositol phospholipid-anchored membrane-proteins—a further definition of micrometer scale membrane domains. *J. Cell Biol.* 112:1143–1150.
9. Edidin, M., M. C. Zuniga, and M. P. Sheetz. 1994. Truncation mutants define and locate cytoplasmic barriers to lateral mobility of membrane-glycoproteins. *Proc. Natl. Acad. Sci. USA.* 91:3378–3382.
10. Gheber, L. A., and M. Edidin. 1999. A model for membrane patchiness: lateral diffusion in the presence of barriers and vesicle traffic. *Biophys. J.* 77:3163–3175.
11. Tang, Q., and M. Edidin. 2001. Vesicle trafficking and cell surface membrane patchiness. *Biophys. J.* 81:196–203.
12. Marguet, D., E. T. Spiliotis, T. Pentcheva, M. Lebowitz, J. Schneck, and M. Edidin. 1999. Lateral diffusion of GFP-tagged H2L(d) molecules and of GFP-TAP1 reports on the assembly and retention of those molecules in the endoplasmic reticulum. *Immunity.* 11:231–240.
13. Axelrod, D. 1989. Total internal-reflection fluorescence microscopy. *Methods Cell Biol.* 30:245–270.
14. Yokosuka, T., K. Sakata-Sogawa, W. Kobayashi, M. Hiroshima, A. Hashimoto-Tane, M. Tokunaga, M. L. Dustin, and T. Saito. 2005. Newly generated T cell receptor microclusters initiate and sustain T cell activation by recruitment of Zap70 and SLP-76. *Nat. Immunol.* 6: 1253–1262.